The EMBO Journal Vol. 20 No. 20 pp. 5595–5602, 2001

Exploration of the pore structure of a peptide-gated Na^+ channel

Mallorie Poët, Michel Tauc, Eric Lingueglia[1], Peggy Cance, Philippe Poujeol, Michel Lazdunski[1] and Laurent Counillon[2]

Laboratoire de Physiologie Cellulaire et Moléculaire, CNRS UMR6548, Université de Nice–Sophia Antipolis, Faculté des Sciences, Parc Valrose, 06108 Nice and [1]Institut de Pharmacologie Moléculaire et Cellulaire, CNRS UMR6097, Université de Nice–Sophia Antipolis, 660 route des Lucioles, 06560 Valbonne, France

[2]Corresponding author
e-mail: counillo@unice.fr

The FMRF-amide-activated sodium channel (FaNaC), a member of the ENaC/Degenerin family, is a homotetramer, each subunit containing two transmembrane segments. We changed independently every residue of the first transmembrane segment (TM1) into a cysteine and tested each position's accessibility to the cysteine covalent reagents MTSET and MTSES. Eleven mutants were accessible to the cationic MTSET, showing that TM1 faces the ion translocation pathway. This was confirmed by the accessibility of cysteines present in the acid-sensing ion channels and other mutations introduced in FaNaC TM1. Modification of accessibilities for positions 69, 71 and 72 in the open state shows that the gating mechanism consists of the opening of a constriction close to the intracellular side. The anionic MTSES did not penetrate into the channel, indicating the presence of a charge selectivity filter in the outer vestibule. Furthermore, amiloride inhibition resulted in the channel occlusion in the middle of the pore. Summarizing, the ionic pore of FaNaC includes a large aqueous cavity, with a charge selectivity filter in the outer vestibule and the gate close to the interior.

Keywords: ENac/Degenerins/FMRF-amide/ligand-gated channel/pore structure/substituted cysteine accessibility method

Introduction

FaNaC is a member of the epithelial Na^+ channel (ENaC)/Degenerin gene family of amiloride-sensitive cationic channels. These channels are involved in a wide variety of physiological functions, such as mechanosensation in *Caenorhabditis elegans* (degenerins; Tavernarakis and Driscoll, 1997), and maintenance of mammalian salt balance and salty taste perception (ENaC; Garty and Palmer, 1997) or acid sensing (acid-sensing ion channels, ASICs; Waldmann and Lazdunski, 1998). Mutations in genes encoding members of this family have been shown to be responsible for genetic disorders such as neurodegeneration in *C.elegans* (Chalfie and Wolinski, 1990; Driscoll and Chalfie, 1991) or chronic hypertension (Liddle's syndrome; Shimkets *et al*., 1994; Hansson *et al*., 1995) and pseudohypoaldosteronism type 1 in man (Chang *et al*., 1996). FaNaC has been discovered in *Helix aspersa* neurons (Green *et al*., 1994; Cottrell, 1997) and it has the unique property to form a Na^+-selective ion channel directly activated by the Phe-Met-Arg-Phe-NH_2 (FMRF-amide) peptide. The functional unit of FaNaC is a homotetramer (Coscoy *et al*., 1998), each subunit consisting of two transmembrane segments connected by a large cysteine-rich loop shown to be extracellular in other ENaC/Degenerin channels (Canessa *et al*., 1994; Renard *et al*., 1994; Lai *et al*., 1996). Although no mammalian FaNaC has yet been isolated, this channel is evolutionarily related to the mammalian ASICs, which are external pH sensors present in brain and in sensory neurons where they are thought to participate in nociception associated with tissue acidosis, for instance in ischemic, damaged or inflamed tissue (Waldmann and Lazdunski, 1998). A functional modulation of certain ASIC channels by FMRF-amide and related peptides was recently described (Askwith *et al*., 2000). Due to its unique properties, we decided to use FaNaC as a model system to learn more about the structure–function relationships of the ligand-gated channels belonging to the ENaC/Degenerin gene family.

We used the substituted-cysteine accessibility method (Akabas *et al*., 1992) to investigate the participation of the first transmembrane segment in the ion pore of FaNaC. Each residue of the first transmembrane segment has been substituted individually into a cysteine, and each functional mutant has been exposed to methanethiosulfonates (MTS), i.e. polar cysteine covalent reagents. These hydrophilic molecules can only modify cysteines situated in the aqueous lumen of the channel, because these reagents are charged, and because their reactivity is negligible for thiol groups exposed to a non-polar environment (for review see Karlin and Akabas, 1998). Therefore, this method allows the identification of the residues of transmembrane segments lining the ion translocation pathway. In addition, the pattern of modification provides clues to the secondary structure of these segments. This procedure can also be applied to the TM2. However, its high level of conservation suggests that the systematic substitution of residues into cysteines would lead to the generation of many inactive mutants. The obtainment of 11 inactive cysteine mutants of TM2 in an independent work (M.Poët, P.Cance and L.Counillon, unpublished results) confirms this assumption. In contrast, the high tolerance of TM1 for amino acid substitutions enabled us to use this segment as a reporter for the characterization of the FaNaC ion pore.

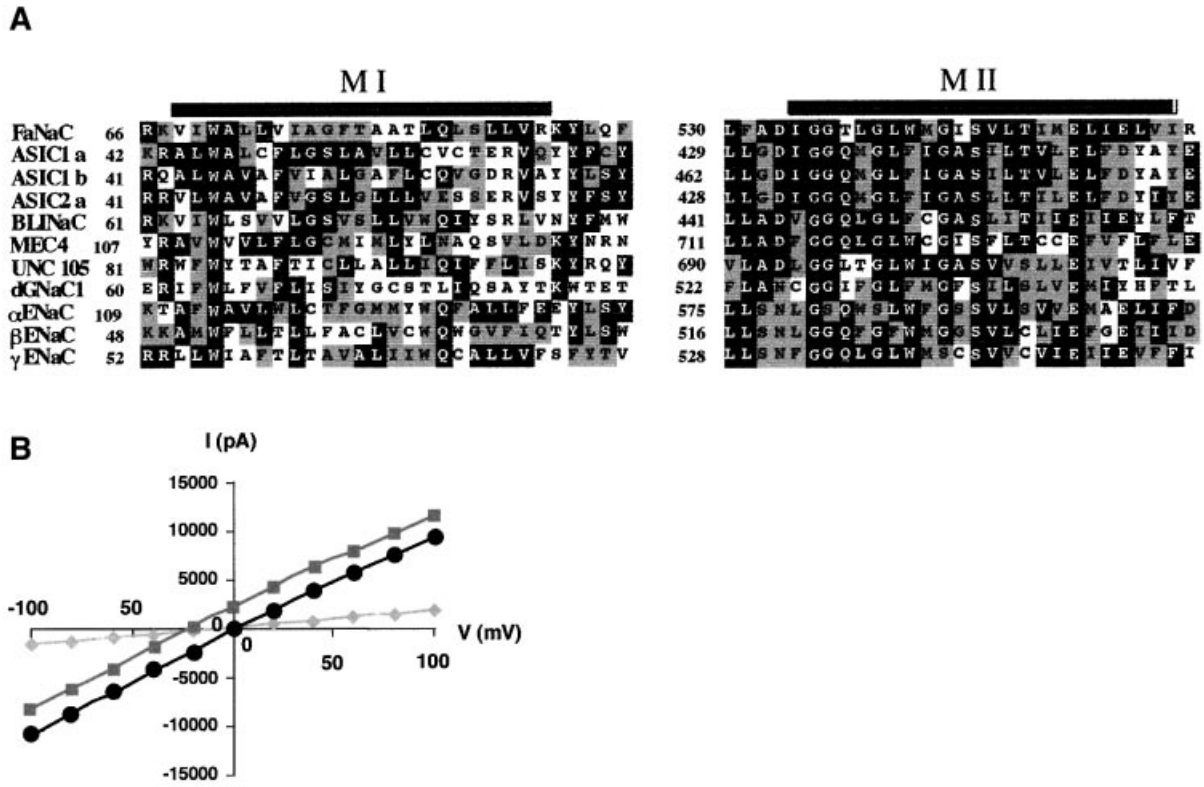

Fig. 1. (**A**) Sequence alignments for TM1 and TM2 regions within different members of the ENaC/Degenerin gene family. The alignment was obtained with the GCG Pileup program. Identical and similar residues are printed white on black and white on gray, respectively. Acid-sensing ion channels (ASICs), brain–liver–intestine amiloride-sensitive Na^+ channel (BLINaC) and epithelial Na^+ channel (ENaC) correspond to the rat sequences; MEC4 and UNC105 are *C.elegans* degenerins and dGNaC1 is a *Drosophila* gonad-specific amiloride-sensitive Na^+ channel. Note the low conservation between the sequences of TM1 when compared with TM2. (**B**) Current–voltage relationship for wild-type FaNaC expressed in HEK293 cells, in the presence of 30 μM FMRF-amide. Cells were maintained in the whole-cell configuration and voltage steps were applied from –100 to +100 mV in 20 mV increments. (Circles) Symmetrical conditions (140 mM NaCl, 0 mM KCl pH 7.4) between intracellular and extracellular medium. (Squares) Extracellular medium: 95 mM KCl, 35 mM NaCl; intracellular medium: 140 mM NaCl, 0 mM KCl. (Diamonds) Residual currents in the absence of FMRF-amide. Similar residual currents were observed in the presence of 30 μM FMRF-amide and 100 μM amiloride.

Results

Expression and characterization of wild-type FaNaC

The cDNA encoding FaNaC was introduced in the pIRES-CD8 polycistronic vector, which allows the coexpression of the cell surface marker CD8 and of the cDNA of interest. Two days after transfection, HEK293 cells containing the pIRES-CD8 plasmid encoding the wild-type FaNaC could be detected visually by the binding of anti-CD8 monoclonal antibody-coated beads (Dynal), and were tested using the whole-cell clamp technique. They expressed a typical FMRF-amide-activated amiloride-sensitive sodium conductance with a K_d for FMRF-amide of 1 μM, and a K_i for amiloride of 8 μM, in good agreement with previous data (Lingueglia *et al*., 1995; Coscoy *et al*., 1998). This current, which exhibited a typical current–voltage relationship, was not present in non-transfected cells, and did not exhibit significant desensitization upon repetitive applications of FMRF-amide (Figures 1B and 2).

FaNaC does not contain any cysteine in its two transmembrane segments but 14 conserved cysteines are present in the extracellular loop of each monomer. As shown in Figure 2, the application of 1 mM MTSET, a cationic MTS, to the wild-type channel does not result in any significant modification of the channel activity. This indicates that these cysteines are not accessible, maybe because they form disulfide bridges, or that the covalent modification of accessible extracellular cysteines does not affect channel function.

Accessibility of the positions of TM1 in the closed state of the channel

We substituted individually the 23 amino acids of the FaNaC first transmembrane segment (positions 68–90) with cysteines using double-stranded site-directed mutagenesis (Quickchange Site-Directed Mutagenesis kit; Stratagene), directly on the pIRES-CD8 expression vector. All mutants were functional except the Trp70Cys mutant. This indicates an important role for this residue, which is confirmed by the fact that it is conserved in all the members of this family, such as the ASICs, MEC4, or the α subunit of the epithelial sodium channel (Figure 1A).

The macroscopic electrophysiological properties (current–voltage relationship, FMRF-amide and amiloride sensitivities) of most of the mutants were essentially identical to those of the wild-type channel. It is worth noting that the Ser86Cys mutant, which was fully activated by FMRF-amide, rapidly desensitized with repetitive application of

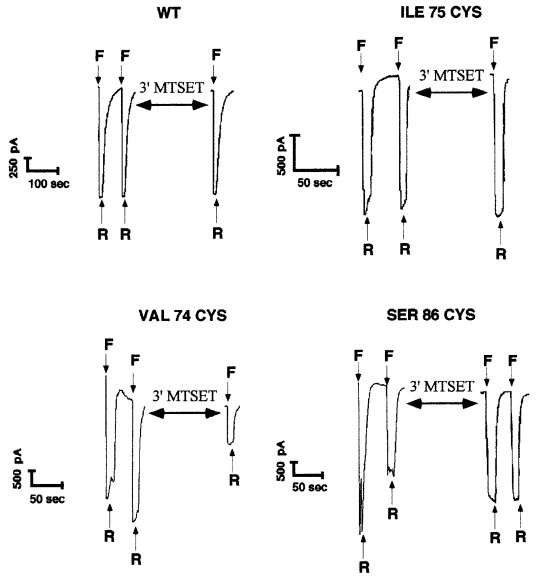

Fig. 2. Susceptibility of wild-type FaNaC and several mutants to 1 mM MTSET. Positive transfectants in the whole-cell clamp configuration were maintained at –40 mV. Bath and pipette solutions were of identical composition (140 mM NaCl, 10 mM HEPES, 1 mM $CaCl_2$ pH 7.4). Cells were briefly perfused twice with the same solution containing 30 μM FMRF-amide to determine the maximal amplitude of the stimulation (I_{max}) before being rinsed until the baseline current was reached, and then perfused with 1 mM MTSET in the same solution for 3 min. The third peak corresponds to the channel stimulation by 30 μM FMRF-amide after 3 min of MTSET application followed by 1 min of rinse. In these conditions, the wild-type channel (WT) and mutants such as Ile75Cys are not affected by 1 mM MTSET, while mutants such as Val74Cys show a marked inhibition. Note that the Ser86Cys mutant, which exhibits a strong desensitization upon FMRF-amide repeated stimulations, regains activity and does not desensitize following 3 min of 1 mM MTSET exposure. F, 30 μM FMRF-amide; R, rinse.

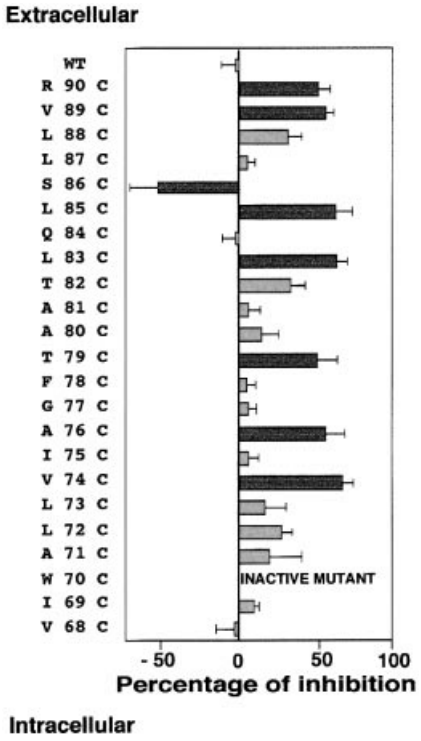

Fig. 3. Histogram summarizing the sensitivities of the cysteine mutants of the FaNaC first transmembrane segment following 3 min of 1 mM MTSET application, and the corresponding SEMs. Experimental procedures were carried out as described in Figure 2 and in Materials and methods. Data for each mutant were obtained from at least six independent recordings and the percentages of inhibition calculated as $(I_{max} - I)/I_{max}$, where I_{max} is the current amplitude before 3 min of MTS application, and I the current amplitude following MTS application. Cysteine mutants at positions 74, 76, 79, 83, 85, 86, 89 and 90 are strongly affected by MTSET (Student's t -test, p <0.001), and the corresponding histogram bars are represented in dark grey.

FMRF-amide (Figure 2). A similar observation was made for mutants Ala71Cys and Leu73Cys.

Mutants such as Val74Cys cannot be fully activated by FMRF-amide following 3 min of MTSET application (Figure 2), indicating that this residue is accessible to the hydrophilic MTSET, and is therefore facing the channel pore. In contrast, Ile75Cys is unaffected by the same treatment (Figure 2), indicating that this position does not face the channel pore. All the mutants were tested under the same conditions. The compilation and statistical analysis of the results revealed two classes of mutants: (i) mutants that were significantly inhibited by MTSET (Student's t-test, p <0.001), with percentages of inhibition equal or superior to 50%; and (ii) mutants considered as not significant with a lower sensitivity to MTSET (<30%). The histogram presented in Figure 3 shows that positions 74, 76, 79, 83, 85, 86, 89 and 90 are facing the pore of the ion channel. To confirm these results, we determined the kinetic constants of inhibition of the various mutants by 1 mM MTSET using pulses of FMRF-amide. As shown in Table I, the results obtained are consistent with the percentages of inhibition determined after 3 min of MTSET exposure. Interestingly, the Ser86Cys mutant, which desensitized after FMRF-amide pulses, regained activity and did not desensitize following MTSET application (Figure 2). This results in a negative inhibition value (Figure 3) corresponding to an increase in channel activity caused by the MTSET application, and strongly suggests that this position is also accessible to MTSET.

The effect of MTSET, when applied intracellularly at 1 mM concentration in the patch pipette in whole-cell configuration, was tested from positions 68 to 74. As shown in Table II the rate constants determined for the cysteine mutants engineered at positions 68, 71, 72 and 74 are comparable to those of other unaffected positions such as 84 and 77 shown in Table I. Thus, we conclude that these positions are not accessible to intracellular MTSET in the closed conformation of the channel. In contrast, the Ile69Cys mutant exhibits a rate constant of inhibition one order of magnitude greater than those of the previously discussed mutants. This shows that position 69 is accessible to intracellular MTSET.

Accessibility of the positions of TM1 in the open state of the channel

We tested the MTSET accessibility of various mutants from position 68 to 90 in the presence of FMRF-amide, i.e. in the open state of the channel. This set of experiments was made possible by the fact that, apart from Ala71Cys, Leu73Cys, Leu85Cys and Ser86Cys, all our MTSET-sensitive mutants did not significantly desensitize during continuous FMRF-amide application. Remarkably, position 72, which is affected only to a negligible extent in the

Table I. Compilation of the kinetic constants of inhibition by 1 mM extracellular MTSET in the closed and open state

Position	Rate of inhibition in the closed state (mM^{-1} s^{-1})	Rate of inhibition in the open state (mM^{-1} s^{-1})
89	0.23 ± 0.05	0.31 ± 0.042
85	0.352 ± 0.13	0.29 ± 0.018
84	0.04 ± 0.03	0.034 ± 0.007
79	0.423 ± 0.103	0.29 ± 0.06
77	0.036 ± 0.024	0.07 ± 0.015
76	0.325 ± 0.155	0.34 ± 0.064
74	0.36 ± 0.04	0.29 ± 0.057
72	0.15 ± 0.06	0.47 ± 0.09

Kinetic constants were determined as described in Materials and methods, using 1-min-spaced pulses of 30 μM FMRF-amide for determinations in the closed state and continuous FMRF-amide applications for determinations in the open state. Positions 84 and 77, which are not accessible to MTSET, are shown for comparison with the accessible positions. Note the concordance of the kinetic constants with the global percentages of inhibition shown in Figures 3 and 4, and the difference between the accessibility of position 72 in the closed and open state.

Table II. Compilation of the kinetic constants of inhibition by 1 mM intracellular MTSET in the closed and open state

Position	Rate of inhibition in the closed state (mM^{-1} s^{-1})	Rate of inhibition in the open state (mM^{-1} s^{-1})
74	0.08 ± 0.055	0.09 ± 0.031
72	0.06 ± 0.075	0.17 ± 0.072
71	0.08 ± 0.03	0.36 ± 0.17
69	0.26 ± 0.037	0.12 ± 0.05
68	0.044 ± 0.011	0.099 ± 0.027

Kinetic constants were determined as described in Materials and methods, using 1-min-spaced pulses of 30 μM FMRF-amide for determinations in the closed state and continuous FMRF-amide application for determinations in the open state. Note the differences of accessibility between the closed and open states from position 69 to 72, showing that this region of the channel is involved in the gating mechanism.

closed state, becomes highly accessible in the open state (Figure 4A) when the MTSET is applied extracellularly. This result strongly suggests that the gating mechanism consists of conformational modifications resulting in the opening of a channel constriction located close to its intracellular side. To confirm this hypothesis, we tested the accessibility of positions 68–74 to intracellular MTSET in the open state of the channel. Using this procedure, we discovered that position 69, which is accessible to intracellular MTSET in the closed state of the channel, becomes slightly less sensitive to this reagent upon FMRF-amide application (Table II). Moreover, the cysteines introduced at positions 71 and 72, which were not accessible to intracellular MTSET in the closed state, become significantly affected in the open state. In contrast, position 74, which was not significantly affected by intracellular MTSET in the closed conformation, did not exhibit any detectable increase in its rate of inhibition in the open conformation. The simplest interpretation that can account for this apparently surprising observation is that a constriction situated in the vicinity of Leu72, which is unchanged in the Val74Cys mutant, blocks the accessibility of intracellular MTSET to the upper positions, even in the open state of the channel.

In summary, this set of results shows that the conformational changes leading to the opening of the channel take place in a region of the protein centred around Leu72.

Location of the charge selectivity filter and the amiloride blockage site

To gain information on the charge selectivity filter of the channel, we tested the inhibitory effect of the MTSES MTS on the TM1 cysteine mutants. MTSES is negatively charged and has a steric hindrance comparable to that of MTSET. No significant inhibition could be detected for positions 68–88 (Figure 5). In contrast, positions 89 and 90, which are located in the outer vestibule of the channel, are accessible to the anionic reagent. Therefore, FaNaC discriminates between cationic and anionic MTSs in a region situated in the pore entrance, between positions 85 and 89. Although other effects than accessibility could be responsible for these observations, these results suggest that the charge selectivity filter of the channel might be situated in the vestibule of the ion pore.

The diuretic amiloride is a classical inhibitor of ion channels of the ENaC/Degenerin family. Many data suggest that amiloride blocks these channels by occluding the ion pore (Palmer and Andersen, 1989). To gain access into the amiloride inhibition mechanism of FaNaC, we took advantage of our MTEST-accessible mutants to investigate whether amiloride could protect them from the covalent inhibitor. Continuous addition of amiloride on FaNaC, when activated by FMRF-amide, results in channel inactivation lasting after the inhibitor has been removed. Therefore, we investigated the potential protective effect of amiloride in the closed state of FaNaC. The Val74Cys, Ala76Cys and Thr79Cys MTSET-sensitive mutants are protected by amiloride, when added at a 100 μM concentration together with 1 mM MTSET (Figure 5). In contrast, the Leu83Cys to Arg90Cys MTSET-sensitive mutants are not protected in the same conditions. Amiloride may occlude the pore at a position located between Leu83 and Thr79, i.e. in the close vicinity of the conformational transition between the predicted α-helical and extended region of TM1. However, we cannot exclude the possibility that the binding of amiloride on a site situated apart from the ion pore may produce a conformational modification resulting in the narrowing of the channel near Thr79.

Accessible cysteines in other members of the ENaC/Degenerin family

Our results show that several residues of TM1 face the ion pore of FaNaC, which is constituted by a large aqueous cavity. To investigate whether these conclusions could be extended to other members of the family, we took advantage of the observation that ASIC1a and ASIC1b both have cysteines in their TM1 at positions corresponding to accessible positions in FaNaC (positions 83 and 85). As shown in Figure 6, these two channels are importantly affected by the MTSET treatment (2.5 mM for 5 min). Conversely, the rat ASIC2a channel, which does not

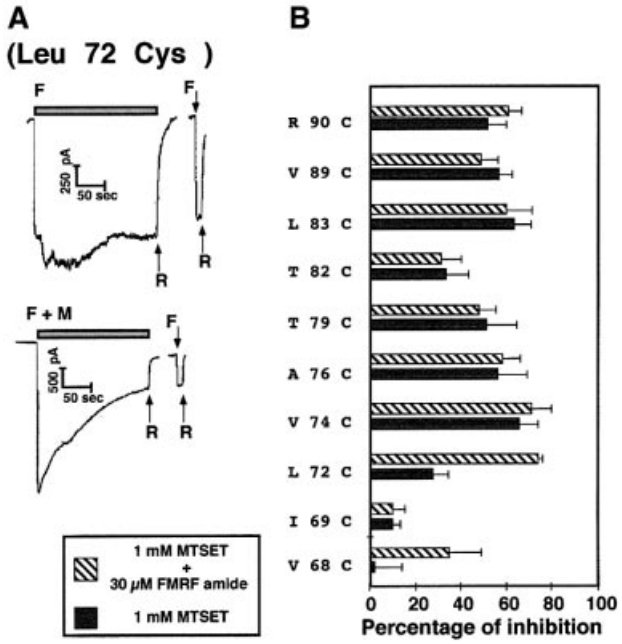

Fig. 4. (**A**) Open channel measurements for the Leu72Cys mutant. Positive transfectants in the whole-cell clamp configuration were maintained at –40 mV with the same bath and pipette solution (140 mM NaCl, 10 mM HEPES, 1 mM $CaCl_2$ pH 7.4). Following one rapid stimulation with 30 μM FMRF-amide, the clamped cells were perfused for 3 min with 30 μM FMRF-amide plus or minus 1 mM MTSET. Note the stability of the FMRF-amide-evoked current, and its exponential decay in the presence of MTSET. F, 30 μM FMRF; R, rinse; M, 1 mM MTSET. The same protocol has been applied for all the mutants that were shown to be accessible to MTSET in the closed configuration, and the recordings are similar, apart from mutants Ala71Cys, Leu85Cys and Ser86Cys, which inactivated upon continuous FMRF-amide stimulation. (**B**) Histogram summarizing the sensitivity of the mutants to 1 mM MTSET in the presence and absence of FMRF-amide. Experimental procedures were carried out as described in (A), and the results were compiled from at least six independent experiments, as described in the legend to Figure 3 and in Materials and methods. Note that the percentages of inhibition are similar in the open and closed configuration, apart from position 72, which becomes unmasked upon channel opening.

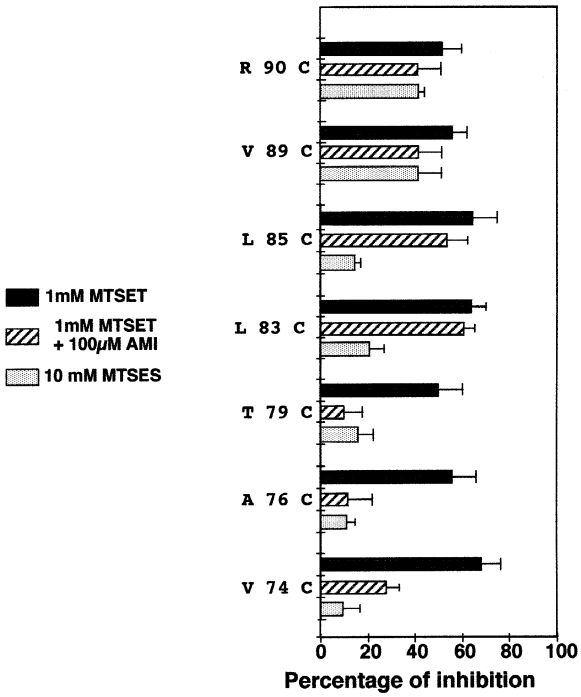

Fig. 5. Mapping of the charge selectivity filter and amiloride blockage positions. This histogram shows the accessibility of the MTSET-sensitive mutants to the anionic 10 mM MTSES in the closed configuration and the protection from 1 mM MTSET inhibition by 100 μM amiloride. For MTSES accessibility, the experimental procedure is the same as in Figure 2, with 10 mM MTSES replacing 1 mM MTSET. For amiloride protection, clamped cells were tested for FMRF-amide activation, perfused with a 100 μM amiloride solution for 3 min, rinsed, and the response to FMRF-amide was re-tested. This allowed us to verify that amiloride could be rinsed efficiently in the closed configuration. The amiloride solution was then switched after 30 s to 100 μM amiloride plus 1 mM MTSET for 3 min. The cells were then rinsed and tested for residual FMRF-amide activation. For comparison, 1 mM MTSET inhibition of the various mutants in the closed configuration is shown on the same graph.

possess any cysteine in its transmembrane region is practically insensitive to MTSET (2.5 mM for 5 min). When Val58 corresponding to Leu83 of FaNaC is mutated to cysteine (Figure 6, see inset), the mutant becomes significantly affected by MTSET. Taken together, the results obtained with the ASIC1a, 1b and 2a proteins suggest some similarity in the exposure of FaNaC and ASICs first transmembrane segment to pore lumen. However, slight structural differences may exist between these two classes of channels as illustrated by the ASIC2a Phe49Cys mutant. This position located deeper in the pore was not affected by the MTS reagent although the corresponding Val74Cys FaNaC mutant was highly sensitive to MTSET, suggesting that the interior of the ion pore is narrower in the proton-gated ion channels than in the FMRF-amide-activated channel.

Substitutions of key residues in TM1

We introduced several amino acid substitutions at three accessible positions situated, respectively, in the extracellular, middle and gating regions of TM1 (positions 89, 79 and 72). The mutated cDNAs were expressed in HEK293 cells and the effect of the introduced changes was evaluated in terms of function and ion selectivity of the mutated channels. The results obtained are shown in Table III. FaNaC TM1 is tolerant to substitutions that do not drastically change the nature of the residues at the above-mentioned positions. In contrast, more important mutations totally impair the functional expression of the channel. Remarkably, the Leu72Phe substitution results in a significant increase of the selectivity of the channel for sodium versus potassium ($pNa^+/pK^+ = 4.96 \pm 0.46$ versus 2.84 ± 0.49 for the wild-type channel). This result confirms the importance of Leu72 in the channel function and gating.

Discussion

This work is the first systematic exploration of the ion pore of a member of the ENaC/Degenerin gene family. In the closed state, nine positions of the first transmembrane segment of FaNaC are significantly accessible to the positively charged covalent reagent MTSET. This shows that a large part of the surface of this transmembrane segment is facing the lumen of the channel. This observation is surprising, due to the low conservation of TM1 in the ENaC/Degenerin family (Figure 1A), which

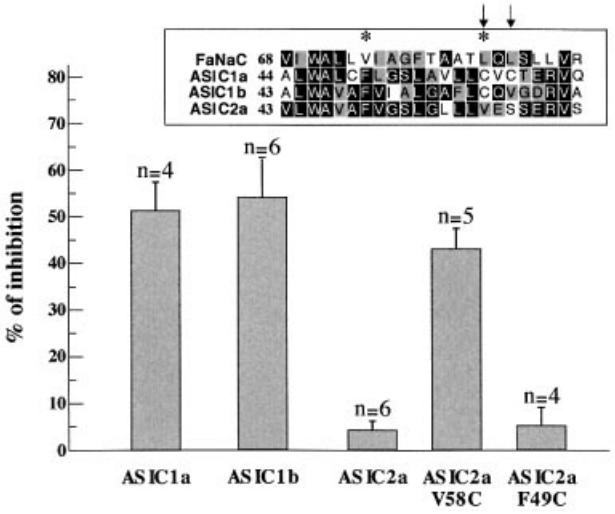

Fig. 6. Effect of MTSET on wild-type and mutated ASICs. Oocytes injected with ASIC1a, ASIC1b and ASIC2a were exposed to MTSET (2.5 mM) for 5 min, and the percentages of inhibition of the H^+-elicited currents were determined as described in Materials and methods. The ASIC1a and 1b isoforms possessing cysteines at positions corresponding to pore-facing residues of FaNaC (see inset) are significantly affected by the sulfhydryl reagent, whilst the ASIC2a isoform, which does not possess any cysteine in its first transmembrane segment is insensitive to MTSET. Introducing a cysteine at position 58 converts ASIC2a into a MTSET-sensitive isoform. However, the cysteine mutant introduced at position 49 (equivalent of position 74 in FaNaC) is not affected by MTSET. The number of oocytes tested in each condition is given above the histograms (mean ± SEM).

led several authors to speculate that this transmembrane segment does not play a key role in ion translocation. However, domain swap experiments have suggested a possible implication of TM1 in the ion pore of the epithelial Na^+ channel (Waldmann *et al*., 1995). To further investigate this point, we engineered various mutations at accessible positions of FaNaC TM1 (Table III), and discovered that introducing several polar or charged residues on the aqueous face of TM1 abolishes the functional expression of the channel. Additionally, we observed that the equivalent of position 83, which is accessible to MTSET in the FaNaC ion pore, is also accessible in the ASIC channels possessing a cysteine at this position (Figure 6). Taken together, these results point out the participation of TM1 in the ion pore of the members of the ENaC/Degenerin family, most of its pore-exposed residues lining passively the ion translocation pathway. Similar conclusions have recently been obtained for another ligand-gated channel sharing a similar topological organization, the $P2X_2$ receptor (Jiang *et al*., 2001).

The analysis of the accessibility pattern of the TM1 cysteine mutants in the absence of FMRF-amide shows that residues situated deeply in the channel pore are accessible in the closed state. This points to the gate of the channel possibly being located near its intracellular face. If this is correct, inaccessible positions situated deeper in the pore will become unmasked upon channel activation. To gain information on the dynamics of the channel gating we repeated our accessibility experiments in the presence of FMRF-amide, i.e. in the open state of the channel.

Table III. Amino acid substitutions at key residues of FaNaC TM1

Residue	Substitution	pNa^+/pK^+
Wild type	none	2.84 ± 0.49
Val89	arginine	inactive
	lysine	2.14 ± 0.41
	tyrosine	2.36 ± 0.54
Thr79	phenylalanine	2.67 ± 0.24
	aspartic acid	inactive
Leu72	glycine	2.48 ± 0.24
	phenylalanine	4.96 ± 0.46
	tyrosine	inactive
	aspartic acid	inactive

Various substitutions were introduced by site-directed mutagenesis, and the corresponding mutants were tested for their functional expression, and selectivity between sodium and potassium (pNa^+/pK^+). Note the presence of several inactive mutants for each tested position, and the change of relative permeability observed for the Leu72Phe mutant.

When MTSET is applied extracellularly, position 72, which was inaccessible in the closed state, becomes unmasked upon channel activation. Symmetrically, when MTSET is applied intracellularly, positions 71 and 72 become accessible in the open state, but the covalent inhibitor cannot reach position 74 (Table II). These results locate the gate of the channel at a highly constricted region centred around Leu72. Additionally, the intracellular position 69, which was significantly affected by MTSET in the closed state of the channel, becomes slightly less accessible in the presence of FMRF-amide (Table II).

As shown in Figure 4B and Table I, the other MTSET-sensitive mutants remain accessible to extracellular MTSET in the open state, suggesting that the gating mechanism does not involve a large modification of the pore conformation, such as rotation of TM1 along its main axis.

The inhibition pattern from Thr79 to the end of the transmembrane segment suggests a 3.6 residues/turn α-helical structure. In contrast, the accessibility of the stretch of sequence between Ala76 and Ile69 suggests a more extended structure. Such a coexistence of different accessibility patterns in transmembrane segments has been observed using a similar technique for other ligand-gated channels, such as the nicotinic acetylcholine receptor (Akabas *et al*., 1992; Zhang and Karlin, 1997). Interestingly, the non-helical region of FaNaC TM1 coincides with the localization of the channel gate, suggesting that the conformational flexibility provided by this unusual structure is involved in the gating mechanism. Alternatively, this non-α-helical organization of the polypeptide chain may leave free backbone carbonyls available for the precise coordination of permeant cations, as is the case for the pore domain of potassium channels. Consistent with this hypothesis, substituting Leu72 by a bulkier phenylalanine significantly increases the channel selectivity for sodium versus potassium (Table III). A similar organization is likely for the other members of the family, since it has been observed that a domain located in the pre-TM1 region is involved in the ion selectivity of some ASIC channels (Coscoy *et al*., 1999).

This work provides the first evidence that the first transmembrane segment of an ENaC/Degenerin ion channel, i.e. the peptide-gated FaNaC, lines the ion

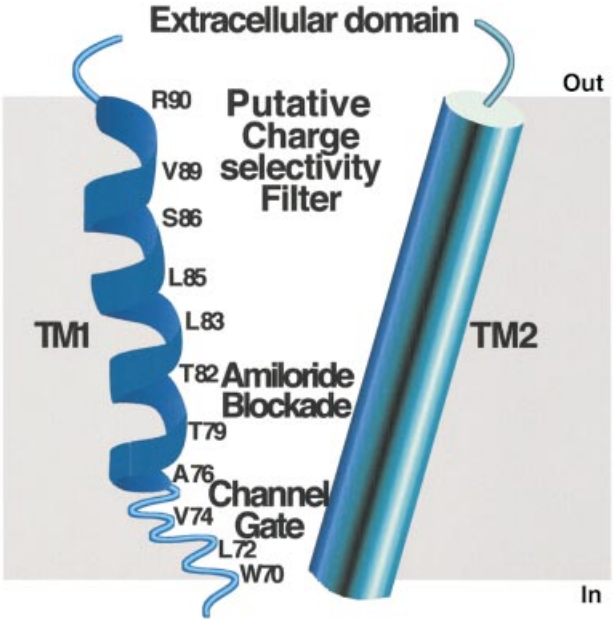

Fig. 7. Schematic representation of the ion pore of FaNaC deduced from the substituted cysteine accessibility method experiments. For simplicity, only one subunit is represented, and TM2 is symbolized by a cylinder.

translocating pathway. A partial model for the FaNaC ion pore, and possibly for the pore of related channels like the proton-gated channel ASICs (Figure 6), which are probably involved in nociception (Waldmann *et al*., 1997; Waldmann and Ladzunski, 1998; Benson *et al*., 1999), emerges from our results and reveals novel features of the channel. This model (Figure 7) has a channel gate situated on the intracellular side, and shows structural transitions in a hinge region of the channel. The accessibility to the rather large MTSET, the localization of the channel gate and the location of the amiloride blockage site all suggest the presence of a large cavity followed by a narrower region opening on the intracellular side. Such functional regions have also been discovered in the two transmembrane domain tetrameric K^+ channel KcsA (Doyle *et al*., 1998; Perozo *et al*., 1999), although in a different organization.

Materials and methods

Cell culture and expression

HEK293 cells were grown on plates coated with collagen in Dulbecco's modified Eagle's medium supplemented with 50 mg/ml streptomycin, 50 U/ml penicillin and 10% fetal calf serum at 37°C, in a humidified atmosphere of 5% CO_2 and 95% air. The cDNA encoding FaNaC was introduced in a polycistronic expression vector derived from the pIRESneo plasmid (CMV promoter; Clontech), in which the neomycin resistance gene has been replaced by the cDNA encoding the α chain of the human CD8 cell surface antigen. Transfected cells coexpress FaNaC and CD8 at their plasma membrane and can be visualized by the binding of anti-CD8-coated latex beads (Dynal) (Jurman *et al*., 1994). 10^5 cells/35mm dish were transfected with 2 μg of plasmid DNA using the DEAE–dextran procedure followed by a 3 h chloroquine shock to inhibit DNA degradation by lysosomal hydrolases (Sambrook *et al*., 1989). 48–72 h after transfection, cells were rinsed and incubated in the 140 mM NaCl medium used for electrophysiological characterization (see below), with 1 μl of anti-CD8-coated latex beads. Transiently transfected cells were localized visually on the patch–clamp set inverted microscope by their ability to bind beads, and tested for their response to FMRF-amide using the whole-cell clamp technique.

Site-directed mutagenesis

Site-directed mutagenesis was performed directly on double-stranded pIREScd8 plasmid DNA (Quickchange Site-Directed Mutagenesis kit; Stratagene) with purified primers (Life Technologies). For the individual substitution of every position of TM1 into a cysteine, the primers were designed to introduce a cysteine substitution at every position of the first transmembrane segment, the TGT or TGC triplets replacing the original codon. For the substitution of positions 72, 79 and 89 into other residues than cysteines, degenerated primers optimized for allowing the desired amino acid substitutions at the appropriate codons (in bold) were used and are listed below (sense primers):

Leu72 Phe/Tyr: 5′-GTC ATC TGG GCA **T(A/T)T** CTG GTG ATC GCC-3′
Leu72 Gly/Asp: 5′-GTC ATC TGG GCA **G(A/G)C** CTG GTG ATC GCC-3′
Thr79 Phe/Tyr: 5′-ATC GCC GGC TTC **T(A/T)T** GCT GCC ACG CTG-3′
Thr79 Gly/Asp: 5′-ATC GCC GGC TTC **G(A/G)C** GCT GCC ACG CTG-3′
Val89 Phe/Tyr: 5′-G TCG CTG CTG **T(A/T)T** AGG AAG TAC CTG-3′
Val89 Lys/Arg: 5′-G TCG CTG CTG **A(A/G)A** AGG AAG TAC CTG-3′

For each mutant, at least four clones obtained from the mutagenesis reaction were sequenced manually or automatically, and two independently mutated clones were transfected and tested for each position.

Electrophysiological characterization of the mutants

Whole-cell currents were recorded from transfected cells maintained at 30°C for the duration of the experiments. For the MTS accessibility studies, the patch pipettes (resistance 2–3 MΩ) were filled with the same solution used for the extracellular medium (140 mM NaCl, 1 mM $CaCl_2$, 5 mM glucose, 10 mM HEPES pH 7.4, plus or minus 1 mM MTSET), and the cells were maintained at a holding potential (V_{hold}) of –40 mV. Current–voltage relations were determined using the same solution as above (without $CaCl_2$) for the patch pipettes, while the extracellular medium was composed of 95 mM KCl, 35 mM NaCl, 5 mM glucose, 10 mM HEPES pH 7.4. Voltage steps of 400 ms duration were applied every 2 s from –100 mV to +100 mV in 20 mV increments. Relative permeability ratios (pNa^+/pK^+) were calculated using the Goldman–Hodgkin–Katz equation. The patch pipette was connected via an Ag/AgCl wire to the Vp500 acquisition system (Biologic). FMRF-amide (Sigma), amiloride (Sigma), MTSET (Toronto Research Chemicals) and MTSES (Toronto Research Chemicals) were diluted in the 140 mM NaCl solution to final concentrations of 30 μM, 100 μM, 1 mM and 10 mM, respectively. When compared with MTSET, MTSES was used at a 10 mM concentration instead of 1 mM, in order to compensate for its lower reactivity with small sulfhydryl compounds. Solutions were perfused in the extracellular bath by using a four-channel glass pipette, the tip of which was placed as close as possible to the clamped cell. To limit the rate of MTS hydrolysis in aqueous solutions (Karlin and Akabas, 1998), these compounds were stored and used extemporaneously according to the vendor's (Toronto Research Chemicals) instructions.

Data analysis

Data were digitized at 1 kHz and visualized with the visual patch 1.14 user interface software (Biologic), and stored on the hard drive for analysis using Biopatch 3.0 and Clampfit softwares (Biologic). For each recording, the percentage of inhibition was calculated as $(I_{max} - I)/I_{max}$, where I_{max} is the average of the current amplitudes before 3 min of MTS pplication, and I the average of the current amplitudes following MTS application. For all the mutants, the responses to 3-min-spaced pulses of FMRF-amide were recorded in order to test for eventual desensitization. Ala71Cys, Leu73Cys and Ser86Cys presented such a phenotype, and for these mutants the desensitization percentage was subtracted from the inhibition percentage observed after 3 min of MTS application. For all the positions tested, the current values obtained from at least six independent complete recordings were averaged to calculate the mean percentages of inhibition, and the corresponding SEM. The significance of the differences between the average inhibition was determined using the Student's *t*-test (SigmaStat 1.0). Kinetic constants of inhibition were obtained by fitting the inhibition of the FMRF-amide-elicited currents by 1 mM MTSET to single exponentials (SigmaPlot 4.0). The results presented in Tables I and II are the average of at least four independent determinations for each mutant tested.

Effect of MTSET on wild-type and mutated ASICs in Xenopus oocytes

The ASIC2a mutants were prepared using a modification of the method of gene splicing by overlap extension (Horton *et al*., 1989).

Isolation, maintenance and injection of stage V and VI *Xenopus* oocytes with wild-type or mutated ASICs were performed as previously described (Sakai *et al*., 1999). cRNAs were synthesized (Stratagene Kit) using a *Not* I-digested pBSK-SP6-globin vector containing rat ASIC1a or rat ASIC2a (wild type or mutant) and then injected (0.25–1 ng per oocyte). Rat ASIC1b was expressed by nuclear injection of a DNA solution (100 ng/µl). Microelectrode voltage–clamp assays were performed 1–3 days after injections. The ND96 bathing solution contained 96 mM NaCl, 2 mM KCl, 1 mM $MgCl_2$, 1.8 mM $CaCl_2$ and 5 mM HEPES pH 7.4 (with NaOH). The susceptibility of wild-type and mutant ASICs to the MTSET reagent was tested using the following protocol: the ASIC currents were activated by a brief application of pH 6.0 (ASIC1a and ASIC1b) or pH 4.0 (ASIC2a) solutions. The mean amplitude of the current (recorded at a holding potential of –70 mV) before exposure to MTSET (I_{max}) was established by four consecutive applications of the low pH for 5–10 s. Individual applications were separated by wash periods of 2 min. The MTSET (2.5 mM) was then applied for 5 min and washed. The mean current amplitude after exposure to MTSET (I_{MTSET}) was determined with four pH applications following the same procedure. The percentage of inhibition was calculated as $(1 - I_{MTSET}/I_{max}) \times 100$. Statistical analysis was performed as described above.

Acknowledgements

We are grateful to Drs Reinhart, A.F.Reithmeier and Fergus R.McKenzie for critical reading of the manuscript, Rainer Waldmann for fruitful discussions, Michel Bidet for his help, and to Béatrice Jelski for technical assistance in cell culture. This work was supported by the Centre National de la Recherche Scientifique (Programme Biologie Cellulaire, du normal au pathologique 96030).

References

Akabas,M.H., Stauffer,D.A., Xu,M. and Karlin,A. (1992) Acetylcholine receptor channel structure probed in cysteine-substitution mutants. *Science*, **258**, 307–310.

Askwith,C.C., Cheng,C., Ikuma,M., Benson,C., Price,M.P. and Welsh,M.J. (2000) Neuropeptide FF and FMRF-amide potentiate acid-evoked currents from sensory neurons and proton-gated DEG/ENaC channels. *Neuron*, **26**, 133–141.

Benson,C.J., Eckert,S.P. and McCleskey,E.W. (1999) Acid-evoked currents in cardiac sensory neurons: A possible mediator of myocardial ischemic sensation. *Circ. Res.*, **84**, 921–928.

Canessa,C.M., Merillat,A.M. and Rossier,B.C. (1994) Membrane topology of the epithelial sodium channel in intact cells. *Am. J. Physiol.*, **267**, C1682–C1690.

Chalfie,M. and Wolinski,E. (1990) The identification and suppression of inherited neurodegeneration in *Caenorhabditis elegans*. *Nature*, **345**, 410–416.

Chang,S.S. *et al*. (1996) Mutations in subunits of the epithelial sodium channel cause salt wasting with hyperkalaemic acidosis, pseudohypoaldosteronism type 1. *Nature Genet.*, **12**, 248–253.

Coscoy,S., Lingueglia,E., Lazdunski,M. and Barbry,P. (1998) The Phe-Met-Arg-Phe-amide-activated sodium channel is a tetramer. *J. Biol. Chem.*, **273**, 8317–8322.

Coscoy,S., de Weille,J.R., Lingueglia,E. and Lazdunski,M. (1999) The pre-transmembrane 1 domain of acid-sensing ion channels participates in the ion pore. *J. Biol. Chem.*, **274**, 10129–10132.

Cottrell,G.A. (1997) The first peptide-gated ion channel. *J. Exp. Biol.*, **200**, 2377–2386.

Doyle,D.A., Morais Cabral,J., Pfuetzner,R.A., Kuo,A., Gulbis,J.M., Cohen,S.L., Chait,B.T. and MacKinnon,R. (1998) The structure of the potassium channel: molecular basis of K^+ conduction and selectivity. *Science*, **280**, 69–77.

Driscoll,M. and Chalfie,M. (1991) The *Mec-4* gene is a member of a family of *Caenorhabditis elegans* genes that can mutate to induce neuronal degeneration. *Nature*, **349**, 588–593.

Garty,H. and Palmer,L.G. (1997) Epithelial sodium channels: function, structure, and regulation. *Physiol. Rev.*, **77**, 359–396.

Green,K.A., Falconer,S.W. and Cottrell,G.A. (1994) The neuropeptide Phe-Met-Arg-Phe-NH2 (FMRFamide) directly gates two ion channels in an identified Helix neurone. *Pflugers Arch.*, **428**, 232–240.

Hansson,J.H., Nelson-Williams,C., Suzuki,H., Schild,L., Lu,Y., Canessa,C., Iwasaki,T., Rossier,B.C. and Lifton,R.P. (1995) Hypertension caused by a truncated epithelial sodium channel γ subunit: genetic heterogeneity of Liddle syndrome. *Nature Genet.*, **11**, 76–82.

Horton,R.M., Hunt,H.D., Ho,S.N., Pullen,J.K. and Pease,L.R. (1989) Engineering hybrid genes without the use of restriction enzymes: gene splicing by overlap extension. *Gene*, **77**, 61–68.

Jiang,L.H., Rassendren,F., Spelta,V., Surprenant,A. and North,R.A. (2001) Aminoacid residues involved in gating identified in the first membrane spanning domain of the rat $P2X_2$ receptor. *J. Biol. Chem.*, **276**, 14902–14908.

Jurman,M.E., Boland,L.M. and Yellen,G. (1994) Visual identification of individual transfected cells for electrophysiology using antibody-coated beads. *Biotechniques*, **17**, 876–881.

Karlin,A. and Akabas,M.H. (1998) Substituted-cysteine accessibility method. *Methods Enzymol.*, **293**, 123–145.

Lai,C., Hong,K., Kinnell,M., Chalfie,M. and Driscoll,M. (1996) Sequence and transmembrane topology of MEC-4, an ion channel subunit required for mechanotransduction in *Caenorhabditis elegans*. *J. Cell Biol.*, **133**, 1071–1081.

Lingueglia,E., Champigny,G., Lazdunski,M. and Barbry,P. (1995) Cloning of the amiloride-sensitive FMRFamide peptide-gated sodium channel. *Nature*, **378**, 730–733.

Palmer,L.G. and Andersen,O.S. (1989) Interactions of amiloride and small monovalent cations with the epithelial sodium channel. Inferences about the nature of the channel pore. *Biophys. J.*, **55**, 779–787.

Perozo,E., Cortes,D.M. and Cuello,L.G. (1999) Structural rearrangements underlying K^+-channel activation gating. *Science*, **285**, 73–78.

Renard,S., Lingueglia,E., Voilley,N., Lazdunski,M. and Barbry,P. (1994) Biochemical analysis of the membrane topology of the amiloride-sensitive Na^+ channel. *J. Biol. Chem.*, **269**, 12981–12986.

Sakai,H., Lingueglia,E., Champigny,G., Mattei,M.G. and Lazdunski,M. (1999) Cloning and functional expression of a novel degenerin-like Na^+ channel gene in mammals. *J. Physiol. (Lond.)*, **519**, 323–333.

Sambrook,J., Fritsch,E.F. and Maniatis,T. (1989) *Molecular Cloning: A Laboratory Manual*. 2nd edn. Cold Spring Harbor Laboratory Press, Cold Spring Harbor, NY.

Shimkets,R.A. *et al*. (1994) Liddle's syndrome: heritable human hypertension caused by mutations in the beta subunit of the epithelial sodium channel. *Cell*, **79**, 407–414.

Tavernarakis,N. and Driscoll,M. (1997) Molecular modeling of mechanotransduction in the nematode *Caenorhabditis elegans*. *Annu. Rev. Physiol.*, **59**, 659–689.

Waldmann,R. and Lazdunski,M. (1998) H^+ -gated cation channels: neuronal acid sensors in the NaC/DEG family of ion channels. *Curr. Opin. Neurobiol.*, **8**, 418–424.

Waldmann,R., Champigny,G. and Lazdunski,M. (1995) Functional degenerin-containing chimeras identify residues essential for amiloride-sensitive Na^+ channel function. *J. Biol. Chem.*, **270**, 11735–11737.

Waldmann,R., Champigny,G., Bassilana,F., Heurteaux,C. and Lazdunski,M. (1997) A proton-gated cation channel involved in acid sensing. *Nature*, **386**, 173–177.

Zhang,H. and Karlin,A. (1997) Identification of the acetylcholine receptor channel-lining residues in the M1 segment of the β subunit. *Biochemistry*, **36**, 15856–15864.

Received August 21, 2000; revised July 2, 2001; accepted August 31, 2001